

Analytic Implementations of the Cardinalized Probability Hypothesis Density Filter

Ba-Tuong Vo, Ba-Ngu Vo, and Antonio Cantoni, *Fellow, IEEE*

Abstract—The probability hypothesis density (PHD) recursion propagates the posterior intensity of the random finite set (RFS) of targets in time. The cardinalized PHD (CPHD) recursion is a generalization of the PHD recursion, which jointly propagates the posterior intensity and the posterior cardinality distribution. In general, the CPHD recursion is computationally intractable. This paper proposes a closed-form solution to the CPHD recursion under linear Gaussian assumptions on the target dynamics and birth process. Based on this solution, an effective multitarget tracking algorithm is developed. Extensions of the proposed closed-form recursion to accommodate nonlinear models are also given using linearization and unscented transform techniques. The proposed CPHD implementations not only sidestep the need to perform data association found in traditional methods, but also dramatically improve the accuracy of individual state estimates as well as the variance of the estimated number of targets when compared to the standard PHD filter. Our implementations only have a cubic complexity, but simulations suggest favorable performance compared to the standard Joint Probabilistic Data Association (JPDA) filter which has a nonpolynomial complexity.

Index Terms—Cardinalized probability hypothesis density (CPHD) filter, multitarget Bayesian filtering, multitarget tracking, probability hypothesis density (PHD) filter, random finite sets (RFSs).

I. INTRODUCTION

THE objective of multitarget tracking is to simultaneously estimate the time-varying number of targets and their states from a sequence of observation sets in the presence of data association uncertainty, detection uncertainty, and noise. The random finite set (RFS) approach, introduced by Mahler as finite set statistics (FISST) [1], [2] is an elegant formulation of the multitarget tracking problem which has generated substantial research interest [3]–[19]. In essence, the collection of target states at any given time is treated as a set-valued multitarget state, and the corresponding collection of sensor measurements is treated as a set-valued multitarget observation. Using RFSs to model the multitarget state and observation, the multitarget tracking problem can be formulated in a Bayesian filtering framework

by propagating the posterior distribution of the multitarget state in time [2], [3].

Due to the inherent combinatorial nature of multitarget densities and the multiple integrations on the (infinite dimensional) multitarget state and observation spaces, the multitarget Bayes recursion is intractable in most practical applications [2], [3]. To alleviate this intractability, the probability hypothesis density (PHD) recursion [2] was developed as a first moment approximation to the multitarget Bayes recursion. The PHD recursion in fact propagates the posterior intensity of the RFS of targets in time. The PHD recursion has the distinct advantage that it operates only on the single-target state space and avoids data associations. Contrary to the belief that the PHD recursion is intractable [20], a closed-form solution for linear Gaussian models was proposed in [4], and a full sequential Monte Carlo (SMC) implementation was proposed in [3] with relevant convergence results established in [3], [15], and [16]. Multitarget filters based on the PHD recursion have since found successful application in a host of practical problems, for example, terrain vehicle tracking [5], radar tracking [6], feature point tracking of image sequences [7], bistatic radar tracking [8], and sonar image tracking [9], [21]. Novel extensions of the PHD recursion have also been proposed in [19] for multiple models, and in [12], [13], [22], and [23] for performing track estimation.

The PHD recursion propagates cardinality information with only a single parameter (the mean of the cardinality distribution), and thus, it effectively approximates the cardinality distribution by a Poisson distribution. Since the mean and variance of a Poisson distribution are equal, when the number of targets present is high, the PHD filter estimates the cardinality with a correspondingly high variance. In practice, this limitation manifests itself in erratic estimates of the number of targets [11]. To address this problem, in [24] and [25], Mahler relaxed the first-order assumption on the number of targets and derived a generalization of the PHD recursion known as the cardinalized PHD (CPHD) recursion, which jointly propagates the intensity function and the cardinality distribution (the probability distribution of the number of targets). The pressing question is: Does the additional propagation of cardinality information improve the accuracy of multitarget state estimates? The answer to this question hinges on solving the CPHD recursion. So far, however, no closed-form solutions for the CPHD recursion have been established [24], [25].

The key contribution of this paper is a *closed-form solution to the CPHD recursion for linear Gaussian multitarget models*. Based on this solution, we also develop the following:

- an efficient filter for tracking an unknown time-varying number of targets in clutter (Sections III and IV);

Manuscript received August 14, 2006; revised November 13, 2006. The associate editor coordinating the review of this manuscript and approving it for publication was Dr. Marcelo G. S. Bruno. This work was supported in part by the Australian Telecommunications Cooperative Research Centre and by the Australian Research Council under the Discovery Grant DP0345215.

B.-T. Vo and A. Cantoni are with the Western Australian Telecommunications Research Institute, The University of Western Australia, Crawley, WA 6009, Australia (e-mail: vob@watri.org.au; cantoni@watri.org.au).

B.-N. Vo is with the Department of Electrical and Electronic Engineering, The University of Melbourne, Parkville, Vic. 3010, Australia (e-mail: bv@ee.unimelb.edu.au).

Digital Object Identifier 10.1109/TSP.2007.894241

- a reduced complexity filter for tracking a known fixed number of targets in clutter (Section V);
- extensions of the proposed closed-form recursion to accommodate nonlinear multitarget models using linearization and unscented transform techniques (Section VI).

Our proposed multitarget filter is a generalization of the Gaussian mixture PHD filter described in [4]. Although both filters propagate Gaussian mixture intensities analytically in time, there are two key differences. First, the intensity propagation equation in the CPHD filter is much more complex than that in the PHD filter. Second, in the CPHD filter, there is the additional propagation of the posterior cardinality distribution which is coupled to the propagation of the posterior intensity. Indeed, the Gaussian mixture CPHD filter reduces to the Gaussian mixture PHD filter if the cardinality distributions of the posterior and predicted RFSs are Poisson.

In simulations, our example of tracking an unknown time-varying number of targets in clutter illustrates that an average 12.5 times reduction in the variance of the cardinality estimate of the PHD filter can be obtained. In addition, our example of tracking a known fixed number of targets in clutter illustrates that favorable estimation performance compared to the Joint Probabilistic Data Association (JPDA) filter can be obtained. In the latter comparison, the JPDA filter is run with a gating threshold such that both filters have comparable throughput times.

Preliminary results have been published in previous conference papers; a summary of the closed-form solution has appeared in [26] and a performance comparison with the PHD filter has appeared in [27].

This paper is organized as follows. Section II provides an overview of RFSs, the multitarget Bayes recursion, and the PHD recursion. Then, Section III introduces the CPHD recursion and proposes a closed-form solution to the CPHD recursion for linear Gaussian multitarget models. Demonstrations and numerical studies are considered in Section IV. The reduced complexity filter for tracking a fixed number of targets is derived along with a closed-form recursion for linear Gaussian models in Section V. Nonlinear extensions are proposed in Section VI. Closing remarks are given in Section VII.

II. BACKGROUND

In this section, we review the multitarget tracking problem formulated in the RFS or point process framework. In Section II-A, the central ideas in random set modeling are described and the full multitarget Bayes recursion is presented, and in Section II-B the PHD recursion is presented. This sets the scene for Section III, where the CPHD recursion is considered.

A. RFSs

Suppose at time k there are $N(k)$ targets with states $x_{k,1}, \dots, x_{k,N(k)}$ each taking values in a state space $\mathcal{X} \subseteq \mathbb{R}^{n_x}$. Suppose also at time k that $M(k)$ measurements $z_{k,1}, \dots, z_{k,M(k)}$ are received each taking values in an observation space $\mathcal{Z} \subseteq \mathbb{R}^{n_z}$. Then, the *multitarget state* X_k and the *multitarget measurement* Z_k , at time k , are defined as

$$X_k = \{x_{k,1}, \dots, x_{k,N(k)}\} \in \mathcal{F}(\mathcal{X}) \quad (1)$$

$$Z_k = \{z_{k,1}, \dots, z_{k,M(k)}\} \in \mathcal{F}(\mathcal{Z}) \quad (2)$$

where $\mathcal{F}(\mathcal{X})$ and $\mathcal{F}(\mathcal{Z})$ denote the respective collections of all finite subsets of \mathcal{X} and \mathcal{Z} . By modeling the multitarget state and multitarget observation as RFSs, the multitarget filtering problem can be posed as a Bayesian filtering problem [1]–[3] with state space $\mathcal{F}(\mathcal{X})$ and observation space $\mathcal{F}(\mathcal{Z})$. Intuitively, an RFS is simply a finite-set-valued random variable which can be completely characterized by a discrete probability distribution and a family of joint probability densities. The discrete distribution characterizes the cardinality of the set, while for a given cardinality, an appropriate density characterizes the joint distribution of all elements in the set [1], [28], [29]. In this paper, we consider multitarget dynamics modeled by

$$X_k = \left[\bigcup_{\zeta \in X_{k-1}} S_{k|k-1}(\zeta) \right] \cup \Gamma_k \quad (3)$$

where X_{k-1} is the multitarget state at time $k-1$, $S_{k|k-1}(\zeta)$ is the surviving RFS of target at time k that evolved from a target with previous state ζ , and Γ_k is the RFS of spontaneous births at time k (for simplicity we do not consider target spawning¹). Similarly, the multitarget sensor observations are modeled by

$$Z_k = \left[\bigcup_{x \in X_k} \Theta_k(x) \right] \cup K_k \quad (4)$$

where $\Theta_k(x)$ is the RFS of measurements generated by the single-target state x at time k and K_k is the RFS of clutter measurements or false alarms at time k .

The *multitarget transition density* $f_{k|k-1}(\cdot|\cdot)$ describes the time evolution of the multitarget state and encapsulates the underlying models of target motions, births and deaths. Similarly, the *multitarget likelihood*² $g_k(\cdot|\cdot)$ describes the multitarget sensor measurement and encapsulates the underlying models of detections, false alarms, and target generated measurements. The *multitarget Bayes recursion* propagates the *multitarget posterior density* $\pi_k(\cdot|Z_{1:k})$ in time [1]–[3] according to

$$\begin{aligned} \pi_{k|k-1}(X_k|Z_{1:k-1}) \\ = \int f_{k|k-1}(X_k|X) \pi_{k-1}(X|Z_{1:k-1}) \mu_s(dX) \end{aligned} \quad (5)$$

$$\begin{aligned} \pi_k(X_k|Z_{1:k}) \\ = \frac{g_k(Z_k|X_k) \pi_{k|k-1}(X_k|Z_{1:k-1})}{\int g_k(Z_k|X) \pi_{k|k-1}(X|Z_{1:k-1}) \mu_s(dX)} \end{aligned} \quad (6)$$

where μ_s is an appropriate reference measure on $\mathcal{F}(\mathcal{X})$. For further details on a measure theoretic description of the multitarget Bayes recursion, the reader is referred to [3]. However, due to the combinatorial nature of multitarget densities and the multiple integrations in (5) and (6), the multitarget Bayes recursion is intractable in most practical applications.

¹Generally, the RFS framework for multiobject filtering encompasses target spawning; for further details, see [2].

²The same notation is used for multitarget and single-target densities throughout. There should be no conflict since in the single-target case the arguments are vectors whereas in the multitarget case the arguments are finite sets.

B. PHD Recursion

The PHD or the *intensity function* of an RFS X on \mathcal{X} , is a nonnegative function v on \mathcal{X} with the property that for any closed subset $S \subseteq \mathcal{X}$

$$\mathbb{E}[|X \cap S|] = \int_S v(x) dx$$

where $|X|$ denotes the number of elements of X . In other words, for a given point x , the intensity $v(x)$ is the density of expected number of targets per unit volume at x . Indeed, the intensity function is the first-order moment of an RFS [28], [29].

An important class of RFSs are the *Poisson* RFSs, which are completely characterized by their intensity function. They have the unique property that the distribution of the cardinality of X is Poisson with mean $N = \int v(x) dx$, and for a given cardinality the elements of X are independent and identically distributed (i.i.d.) with probability density v/N . More generally, an RFS whose elements are i.i.d. according to v/N , but has arbitrary cardinality distribution, is called an *i.i.d. cluster process* [29].

The PHD recursion was proposed by Mahler in [2] as a first moment approximation to the full multitarget Bayes recursion (5) and (6). It propagates the posterior intensity of the RFS of targets in time and does not require any data association computations. Let $v_{k|k-1}$ and v_k denote the intensities associated with the predicted and posterior multitarget state. Then, based on the following assumptions:

- each target evolves and generates measurements independently of one another;
- the birth RFS and the surviving RFSs are independent of each other;
- the clutter RFS is Poisson and independent of the measurement RFSs;
- the predicted multitarget RFS is Poisson;

the *PHD recursion* is given by

$$\begin{aligned} v_{k|k-1}(x) &= \int p_{S,k}(\zeta) f_{k|k-1}(x|\zeta) v_{k-1}(\zeta) d\zeta + \gamma_k(x) \quad (7) \\ v_k(x) &= [1 - p_{D,k}(x)] v_{k|k-1}(x) \\ &\quad + \sum_{z \in Z_k} \frac{p_{D,k}(x) g_k(z|x) v_{k|k-1}(x)}{\kappa_k(z) + \int p_{D,k}(\xi) g_k(z|\xi) v_{k|k-1}(\xi) d\xi} \end{aligned} \quad (8)$$

where at time k , $f_{k|k-1}(\cdot|\zeta)$ is the single-target transition density given previous state ζ , $p_{S,k}(\zeta)$ is the probability of target existence given previous state ζ , $\gamma_k(\cdot)$ is the intensity of target births, Z_k is the multitarget measurement set, $g_k(\cdot|x)$ is the single-target measurement likelihood given current state x , $p_{D,k}(x)$ is the probability of target detection given current state x , and $\kappa_k(\cdot)$ is the intensity of clutter.

A closed-form solution to the PHD recursion (7) and (8) has been established for linear Gaussian multitarget models; full details on the derivation and implementation are given in [4]. The PHD recursion also encompasses target spawning, however, such provisions are not required here and are omitted for clarity.

The primary weakness of the PHD recursion is a loss of higher order cardinality information. Since the PHD recursion is a first-order approximation, it propagates cardinality

information with only a single parameter and effectively approximates the cardinality distribution by a Poisson distribution with matching mean. Since the mean and variance of a Poisson distribution are equal, when the number of targets present is high, the PHD filter estimates the cardinality with a correspondingly high variance. Additionally, the mean number of targets is effectively an expected *a posteriori* (EAP) estimator, which can be erratic because of minor modes induced by clutter in low signal-to-noise ratio (SNR) conditions.

III. SOLUTION TO THE CPHD RECURSION

The CPHD recursion was proposed by Mahler in [24] and [25] to address the limitations of the PHD recursion. In essence, the strategy behind the CPHD recursion is to jointly propagate the intensity function and the cardinality distribution (the probability distribution of the number of targets). An interesting interpretation of the CPHD recursion was given in [30].

In Section III-A, we derive a special form of the CPHD recursion which explicitly shows the propagation of the intensity and cardinality. This particular form is central to our derivation of a closed-form solution presented in Section III-B. Extraction of multitarget state estimates is described in Section III-C and implementation issues are considered in Section III-D.

The following notation is used throughout the paper. We denote by C_j^ℓ the *binomial coefficient* $(\ell/j!(\ell-j)!)$, P_j^n the *permutation coefficient* $(n!/(n-j)!)$, $\langle \cdot, \cdot \rangle$ the *inner product* defined between two real-valued functions α and β by

$$\langle \alpha, \beta \rangle = \int \alpha(x) \beta(x) dx,$$

(or $\sum_{\ell=0}^{\infty} \alpha(\ell) \beta(\ell)$ when α and β are real sequences), and $e_j(\cdot)$ the *elementary symmetric function* [31] of order j defined for a finite set Z of real numbers by

$$e_j(Z) = \sum_{S \subseteq Z, |S|=j} \left(\prod_{\zeta \in S} \zeta \right)$$

with $e_0(Z) = 1$ by convention.

A. CPHD Recursion

The CPHD recursion rests on the following assumptions regarding the target dynamics and observations:

- each target evolves and generates measurements independently of one another;
- the birth RFS and the surviving RFSs are independent of each other;
- the clutter RFS is an i.i.d. cluster process and independent of the measurement RFSs;
- the prior and predicted multitarget RFSs are i.i.d. cluster processes.

The previous assumptions are similar to those in the PHD recursion, except that in this case, i.i.d. cluster processes are encountered. Let $v_{k|k-1}$ and $p_{k|k-1}$ denote the intensity and cardinality distribution associated with the predicted multitarget state. Let v_k and p_k denote the intensity and cardinality distribution associated with the posterior multitarget state. The following propositions show explicitly how the posterior intensity

and posterior cardinality distribution are jointly propagated in time. (See the Appendix for the proofs.)

Proposition 1: Suppose at time $k-1$ that the posterior intensity v_{k-1} and posterior cardinality distribution p_{k-1} are given. Then, the predicted cardinality distribution $p_{k|k-1}$ and predicted intensity $v_{k|k-1}$ are given by

$$p_{k|k-1}(n) = \sum_{j=0}^n p_{\Gamma,k}(n-j) \Pi_{k|k-1}[v_{k-1}, p_{k-1}](j) \quad (9)$$

$$v_{k|k-1}(x) = \int p_{S,k}(\zeta) f_{k|k-1}(x|\zeta) v_{k-1}(\zeta) d\zeta + \gamma_k(x) \quad (10)$$

where

$$\Pi_{k|k-1}[v, p](j) = \sum_{\ell=j}^{\infty} C_j^{\ell} \frac{\langle p_{S,k}, v \rangle^j \langle 1 - p_{S,k}, v \rangle^{\ell-j}}{\langle 1, v \rangle^{\ell}} p(\ell) \quad (11)$$

$f_{k|k-1}(\cdot|\zeta)$ = single-target transition density at time k
given previous state ζ

$p_{S,k}(\zeta)$ = probability of target existence at time k
given previous state ζ

$\gamma_k(\cdot)$ = intensity of spontaneous births at time k

$p_{\Gamma,k}(\cdot)$ = cardinality distribution of births at time k .

Proposition 2: Suppose at time k that the predicted intensity $v_{k|k-1}$ and predicted cardinality distribution $p_{k|k-1}$ are given. Then, the updated cardinality distribution p_k and updated intensity v_k are given by

$$p_k(n) = \frac{\Upsilon_k^0[v_{k|k-1}, Z_k](n) p_{k|k-1}(n)}{\langle \Upsilon_k^0[v_{k|k-1}, Z_k], p_{k|k-1} \rangle} \quad (12)$$

$$\begin{aligned} v_k(x) &= \frac{\langle \Upsilon_k^1[v_{k|k-1}, Z_k], p_{k|k-1} \rangle}{\langle \Upsilon_k^0[v_{k|k-1}, Z_k], p_{k|k-1} \rangle} \\ &\times [1 - p_{D,k}(x)] v_{k|k-1}(x) \\ &+ \sum_{z \in Z_k} \frac{\langle \Upsilon_k^1[v_{k|k-1}, Z_k \setminus \{z\}], p_{k|k-1} \rangle}{\langle \Upsilon_k^0[v_{k|k-1}, Z_k], p_{k|k-1} \rangle} \\ &\times \psi_{k,z}(x) v_{k|k-1}(x) \end{aligned} \quad (13)$$

where

$$\begin{aligned} \Upsilon_k^u[v, Z](n) &= \sum_{j=0}^{\min(|Z|, n)} (|Z| - j) p_{K,k}(|Z| - j) P_{j+u}^n \\ &\times \frac{\langle 1 - p_{D,k}, v \rangle^{n-(j+u)}}{\langle 1, v \rangle^n} e_j(\Xi_k(v, Z)) \end{aligned} \quad (14)$$

$$\psi_{k,z}(x) = \frac{\langle 1, \kappa_k \rangle}{\kappa_k(z)} g_k(z|x) p_{D,k}(x) \quad (15)$$

$$\Xi_k(v, Z) = \{ \langle v, \psi_{k,z} \rangle : z \in Z \} \quad (16)$$

Z_k = measurement set at time k

$g_k(\cdot|x)$ = single-target measurement likelihood at time k
given current state x

$p_{D,k}(x)$ = probability of target detection at time k
given current state x

$\kappa_k(\cdot)$ = intensity of clutter measurements at time k

$p_{K,k}(\cdot)$ = cardinality distribution of clutter at time k .

Propositions 1 and 2 are, respectively, the prediction and update steps of the CPHD recursion. The CPHD cardinality prediction (9) is simply a convolution of the cardinality distributions of the birth and surviving targets. This is because the predicted cardinality is the sum of the cardinalities of the birth and surviving targets. The CPHD intensity prediction (10) is the same as the PHD prediction (7). Note that the CPHD cardinality and intensity prediction (9)–(10) are uncoupled, while the CPHD cardinality and intensity update (12)–(13) are coupled. Nonetheless, the CPHD intensity update (13) is similar to the PHD update (8) in the sense that both have one missed detection term and $|Z_k|$ detection terms. The cardinality update (12) incorporates the clutter cardinality, the measurement set, the predicted intensity, and predicted cardinality distribution. Indeed, (12) is a Bayes update, with $\Upsilon_k^0[v_{k|k-1}; Z_k](n)$ being the likelihood of the multitarget observation Z_k given that there are n targets, and $\langle \Upsilon_k^0[v_{k|k-1}; Z_k], p_{k|k-1} \rangle$ as the normalizing constant.

B. Closed-Form Solution to the CPHD Recursion

Based on the previous form of the CPHD recursion [see (9), (10), (12), and (13)], we now derive a closed-form solution to the CPHD recursion for the special class of *linear Gaussian multitarget models*.

The class of linear Gaussian multitarget models consists of standard linear Gaussian assumptions for the transition and observation models of individual targets, as well as certain assumptions on the birth, death and detection of targets.

- Each target follows a linear Gaussian dynamical model i.e.,

$$f_{k|k-1}(x|\zeta) = \mathcal{N}(x; F_{k-1}\zeta, Q_{k-1}) \quad (17)$$

$$g_k(z|x) = \mathcal{N}(z; H_k x, R_k) \quad (18)$$

where $\mathcal{N}(\cdot; m, P)$ denotes a Gaussian density with mean m and covariance P , F_{k-1} is the state transition matrix, Q_{k-1} is the process noise covariance, H_k is the observation matrix, and R_k is the observation noise covariance.

- The survival and detection probabilities are state independent, i.e.,

$$p_{S,k}(x) = p_{S,k} \quad (19)$$

$$p_{D,k}(x) = p_{D,k}. \quad (20)$$

- The intensity of the birth RFS is a Gaussian mixture of the form

$$\gamma_k(x) = \sum_{i=1}^{J_{\gamma,k}} w_{\gamma,k}^{(i)} \mathcal{N}(x; m_{\gamma,k}^{(i)}, P_{\gamma,k}^{(i)}) \quad (21)$$

where $w_{\gamma,k}^{(i)}$, $m_{\gamma,k}^{(i)}$, and $P_{\gamma,k}^{(i)}$ are the weights, means, and covariances of the mixture birth intensity.

For the linear Gaussian multitarget model, the following two propositions present a closed-form solution to the CPHD recursion [see (9), (10), (12), and (13)]. More concisely, these propositions show how the posterior intensity (in the form of its Gaussian components) and the posterior cardinality distribution are analytically propagated in time.

Proposition 3: Suppose at time $k-1$ that the posterior intensity v_{k-1} and posterior cardinality distribution p_{k-1} are given, and that v_{k-1} is a Gaussian mixture of the form

$$v_{k-1}(x) = \sum_{i=1}^{J_{k-1}} w_{k-1}^{(i)} \mathcal{N}(x; m_{k-1}^{(i)}, P_{k-1}^{(i)}). \quad (22)$$

Then, $v_{k|k-1}$ is also a Gaussian mixture, and the CPHD prediction simplifies to

$$p_{k|k-1}(n) = \sum_{j=0}^n p_{\Gamma,k}(n-j) \sum_{\ell=j}^{\infty} C_{j,k}^{\ell} p_{k-1}(\ell) p_{S,k}^j (1-p_{S,k})^{\ell-j} \quad (23)$$

$$v_{k|k-1}(x) = v_{S,k|k-1}(x) + \gamma_k(x) \quad (24)$$

where $\gamma_k(x)$ is given in (21)

$$v_{S,k|k-1}(x) = p_{S,k} \sum_{j=1}^{J_{k-1}} w_{k-1}^{(j)} \mathcal{N}(x; m_{S,k|k-1}^{(j)}, P_{S,k|k-1}^{(j)}) \quad (25)$$

$$m_{S,k|k-1}^{(j)} = F_{k-1} m_{k-1}^{(j)} \quad (26)$$

$$P_{S,k|k-1}^{(j)} = Q_{k-1} + F_{k-1} P_{k-1}^{(j)} F_{k-1}^T. \quad (27)$$

Proposition 4: Suppose at time k that the predicted intensity $v_{k|k-1}$ and predicted cardinality distribution $p_{k|k-1}$ are given, and that $v_{k|k-1}$ is a Gaussian mixture of the form

$$v_{k|k-1}(x) = \sum_{i=1}^{J_{k|k-1}} w_{k|k-1}^{(i)} \mathcal{N}(x; m_{k|k-1}^{(i)}, P_{k|k-1}^{(i)}). \quad (28)$$

Then, v_k is also a Gaussian mixture, and the CPHD update simplifies to

$$p_k(n) = \frac{\Psi_k^0[w_{k|k-1}, Z_k](n) p_{k|k-1}(n)}{\langle \Psi_k^0[w_{k|k-1}, Z_k], p_{k|k-1} \rangle} \quad (29)$$

$$v_k(x) = \frac{\langle \Psi_k^1[w_{k|k-1}, Z_k], p_{k|k-1} \rangle}{\langle \Psi_k^0[w_{k|k-1}, Z_k], p_{k|k-1} \rangle} (1 - p_{D,k}) v_{k|k-1}(x) + \sum_{z \in Z_k} \sum_{j=1}^{J_{k|k-1}} w_k^{(j)}(z) \mathcal{N}(x; m_k^{(j)}(z), P_k^{(j)}) \quad (30)$$

where

$$\Psi_k^u[w, Z](n) = \sum_{j=0}^{\min(|Z|, n)} (|Z| - j) p_{K,k}(|Z| - j) P_{j+u}^n \times \frac{(1 - p_{D,k})^{n-(j+u)}}{\langle 1, w \rangle^{j+u}} e_j(\Lambda_k(w, Z)) \quad (31)$$

$$\Lambda_k(w, Z) = \left\{ \frac{\langle 1, \kappa_k \rangle}{\kappa_k(z)} p_{D,k} w^T q_k(z) : z \in Z \right\} \quad (32)$$

$$w_{k|k-1} = [w_{k|k-1}^{(1)}, \dots, w_{k|k-1}^{(J_{k|k-1})}]^T \quad (33)$$

$$q_k(z) = [q_k^{(1)}(z), \dots, q_k^{(J_{k|k-1})}(z)]^T \quad (34)$$

$$q_k^{(j)}(z) = \mathcal{N}(z; \eta_{k|k-1}^{(j)}, S_{k|k-1}^{(j)}) \quad (35)$$

$$\eta_{k|k-1}^{(j)} = H_k m_{k|k-1}^{(j)} \quad (36)$$

$$S_{k|k-1}^{(j)} = H_k P_{k|k-1}^{(j)} H_k^T + R_k \quad (37)$$

$$w_k^{(j)}(z) = p_{D,k} w_{k|k-1}^{(j)} q_k^{(j)}(z) \times \frac{\langle \Psi_k^1[w_{k|k-1}, Z_k], p_{k|k-1} \rangle \langle 1, \kappa_k \rangle}{\langle \Psi_k^0[w_{k|k-1}, Z_k], p_{k|k-1} \rangle \kappa_k(z)} \quad (38)$$

$$m_k^{(j)}(z) = m_{k|k-1}^{(j)} + K_k^{(j)} (z - \eta_{k|k-1}^{(j)}) \quad (39)$$

$$P_k^{(j)} = [I - K_k^{(j)} H_k] P_{k|k-1}^{(j)} \quad (40)$$

$$K_k^{(j)} = P_{k|k-1}^{(j)} H_k^T [S_{k|k-1}^{(j)}]^{-1}. \quad (41)$$

Remark: It was shown in [24] and [25] that the PHD recursion is a special case of the CPHD recursion. Using a similar argument, it can be shown that the Gaussian mixture PHD recursion [4] is a special case of the recursions given by Propositions 3 and 4.

Propositions 3 and 4 can be established by applying the following standard results for Gaussian distributions; for further details on these results, see [4] and the references therein.

Lemma 1: Given F , d , Q , m , and P of appropriate dimensions, and that Q and P are positive definite, $\int \mathcal{N}(x; F\zeta + d, Q) \mathcal{N}(\zeta; m, P) d\zeta = \mathcal{N}(x; Fm + d, Q + FPF^T)$.

Lemma 2: Given H , R , m , and P of appropriate dimensions, and that R and P are positive definite, $\mathcal{N}(z; Hx, R) \mathcal{N}(x; m, P) = q(z) \mathcal{N}(x; \tilde{m}, \tilde{P})$, where $q(z) = \mathcal{N}(z; Hm, R + HPH^T)$, $\tilde{m} = m + K(z - Hm)$, and $\tilde{P} = (I - KH)P$, $K = PH^T(HPH^T + R)^{-1}$.

Proposition 3 is established as follows. The prediction for the intensity is obtained by substituting (17), (19), and (22) into the CPHD intensity prediction (9), and replacing integrals involving products of Gaussian with appropriate Gaussians as given in Lemma 1. The prediction for the cardinality is obtained by using the assumption in (19) to simplify the expression for the CPHD cardinality prediction (10).

Proposition 4 is established as follows. First, (31) is obtained by substituting (18), (20), and (28) into (14), and using Lemma 2 to simplify the resulting expression. The update for the intensity is then obtained by substituting (18), (20), (28), and the result in (31) into the CPHD intensity update (13), and replacing products of Gaussians with appropriate Gaussians as given in Lemma 2. The update for the cardinality is obtained by substituting the result in (31) into the CPHD cardinality update (12).

It follows by induction from Propositions 3 and 4 that if the initial intensity v_0 is a Gaussian mixture (including the case where $v_0 = 0$), then all subsequent predicted intensities $v_{k|k-1}$ and posterior intensities v_k are also Gaussian mixtures. Proposition 3 provides closed-form expressions for computing the means, covariances, and weights of $v_{k|k-1}$ from those of v_{k-1} , and also for computing the distribution $p_{k|k-1}$ from p_{k-1} . Then, Proposition 4 provides closed-form expressions for computing the means, covariances, and weights of v_k from those of $v_{k|k-1}$, and also for computing the distribution p_k from $p_{k|k-1}$, when a new set of measurements arrives. Efficient techniques for computing the elementary symmetric functions are described in Section III-D. Propositions 3 and 4 are, respectively, the prediction and update steps of the CPHD recursion for linear Gaussian multitarget models.

Remark: The previous propositions can easily be extended to linear jump Markov models for handling multiple maneuvering targets analogous to the approach in [19]. However, for reasons of clarity and space constraints, these extensions are omitted.

C. Multitarget State Extraction

Similar to the Gaussian mixture PHD filter [4], state extraction in the Gaussian mixture CPHD filter involves first estimating the number of targets, and then, extracting the corresponding number of mixture components with the highest weights from the posterior intensity as state estimates.

The number of targets can be estimated using, for example, an EAP estimator $\hat{N}_k = \mathbb{E}[X_k]$ or a maximum *a posteriori* (MAP) estimator $\hat{N}_k = \arg \max p_k(\cdot)$. Note that the EAP estimator is likely to fluctuate and be unreliable under low SNR conditions. This occurs because false alarms and target-missed detections tend to induce minor modes in the posterior cardinality, and consequently, the expected value is randomly shifted away from the target-induced primary mode. On the other hand, the MAP estimator is likely to be more reliable since it ignores minor modes and locks directly onto the target-induced primary mode. For these reasons, the MAP estimator is usually preferred over the EAP estimator [24], [25].

Note that the SMC implementation of the PHD filter in [3] can easily be extended to the CPHD case [24], [25]. In SMC implementations, state extraction involves clustering to partition the particle population into a given number of clusters, e.g., the estimated number of targets \hat{N}_k . This works well when the posterior intensity v_k naturally has \hat{N}_k clusters. Conversely, when \hat{N}_k differs from the natural number of clusters in the particle population, the state estimate becomes unreliable. In contrast, the Gaussian mixture representation of the intensities obviates the need for clustering.

D. Implementation Issues

1) *Computing Cardinality Distributions:* Propagating the cardinality distribution essentially involves using (23) and (29) to recursively predict and update the masses of the distribution. However, if the cardinality distribution is infinite tailed, propagation of the entire posterior cardinality is generally not possible since this would involve propagating an infinite number of terms. In practice, if the cardinality distributions are short or moderately tailed, they can be truncated at $n = N_{\max}$ and approximated with a finite number of terms $\{p_k(n)\}_{n=0}^{N_{\max}}$. Such an approximation is reasonable when N_{\max} is significantly greater than the number of targets on the scene at any time.

2) *Computing Elementary Symmetric Functions:* Evaluating the elementary symmetric functions directly from the definition is clearly intractable. Using a basic result from combinatorics theory known as the Newton–Girard formulas or equivalently Vieta’s theorem, the elementary symmetric function $e_j(\cdot)$ can be computed using the following procedure [31]. Let $\rho_1, \rho_2, \dots, \rho_M$ be distinct roots of the polynomial $\alpha_M x^M + \alpha_{M-1} x^{M-1} + \dots + \alpha_1 x + \alpha_0$. Then, $e_j(\cdot)$ for orders $j = 0, \dots, M$ is given by $e_j(\rho_1, \rho_2, \dots, \rho_M) = (-1)^j \alpha_{M-j} / \alpha_M$. The values $e_j(Z)$ can thus be evaluated by expanding out the polynomial with roots given by the elements

of Z , which can be implemented using an appropriate recursion or convolution. For a finite set Z , calculation of $e_j(Z)$ requires $|Z|^2$ operations. It is shown in [32, Th. 8.14] that this complexity can be reduced to $\mathcal{O}(|Z| \log^2 |Z|)$ operations using a suitable decomposition and recursion.

In the CPHD recursion, each data update step requires the calculation of $|Z| + 1$ elementary symmetric functions, i.e., one for Z and one for each set $\{Z \setminus \{z\}\}$ where $z \in Z$. Thus, the CPHD recursion has a complexity of $\mathcal{O}(|Z|^3)$. Furthermore, using the procedure in [32], the CPHD filter has a complexity of $\mathcal{O}(|Z|^2 \log^2 |Z|)$. Although this appears to be a modest saving, when $|Z|$ is large, the reduction in complexity may be of some advantage. In practice, the number of measurements can be reduced by gating techniques as done in traditional tracking algorithms [33], [34].

3) *Managing Mixture Components:* Similar to Gaussian mixture PHD filter [4], the number of Gaussian components required to represent the posterior increases without bound. To mitigate this problem, the “pruning” and “merging” procedure described in [4] is also directly applicable for the Gaussian mixture CPHD filter. The basic idea is to discard components with negligible weights and merge components that are close together. More sophisticated techniques for mixture approximation are available, e.g., [35]; however, these are more computationally expensive.

IV. NUMERICAL STUDIES

In this section, two examples are presented to demonstrate the performance of the proposed Gaussian mixture CPHD filter. Each scenario also presents a performance comparison with the Gaussian mixture PHD filter (see [4] for complete details on this filter), with a view towards investigating the relative advantages and disadvantages of propagating complete cardinality information.

The following single-target model is used in all scenarios. The target state is a vector of position and velocity $x_k = [p_{x,k}, p_{y,k}, \dot{p}_{x,k}, \dot{p}_{y,k}]^T$ and follows a linear Gaussian transition model (17) with

$$F_k = \begin{bmatrix} I_2 & \Delta I_2 \\ 0_2 & I_2 \end{bmatrix} \quad Q_k = \sigma_v^2 \begin{bmatrix} \frac{\Delta^4}{4} I_2 & \frac{\Delta^3}{2} I_2 \\ \frac{\Delta^3}{2} I_2 & \Delta^2 I_2 \end{bmatrix}$$

where I_n and 0_n denote the $n \times n$ identity and zero matrices, respectively, $\Delta = 1s$ is the sampling period, and $\sigma_v = 5 \text{ m/s}^2$ is the standard deviation of the process noise. The probability of target survival is fixed to $p_{S,k} = 0.99$. The single-target measurement model is linear Gaussian (18) with

$$H_k = [I_2 \quad 0_2] \quad R_k = \sigma_\varepsilon^2 I_2$$

where $\sigma_\varepsilon = 10 \text{ m}$ is the standard deviation of the measurement noise. The surveillance region is the square $\mathcal{X} = [-1000, 1000] \times [-1000, 1000]$ (units are in meters). Clutter is modeled as a Poisson RFS with intensity $\kappa_k(z) = \lambda_c V u(z)$, where $u(\cdot)$ is the uniform probability density over \mathcal{X} , $V = 4 \times 10^6 \text{ m}^2$ is the “volume” of \mathcal{X} , and $\lambda_c = 1.25 \times 10^{-5} \text{ m}^{-2}$ is the average clutter intensity (hence, the average number of false detections per frame is 50). The probability of target detection is fixed at $p_{D,k} = 0.98$.

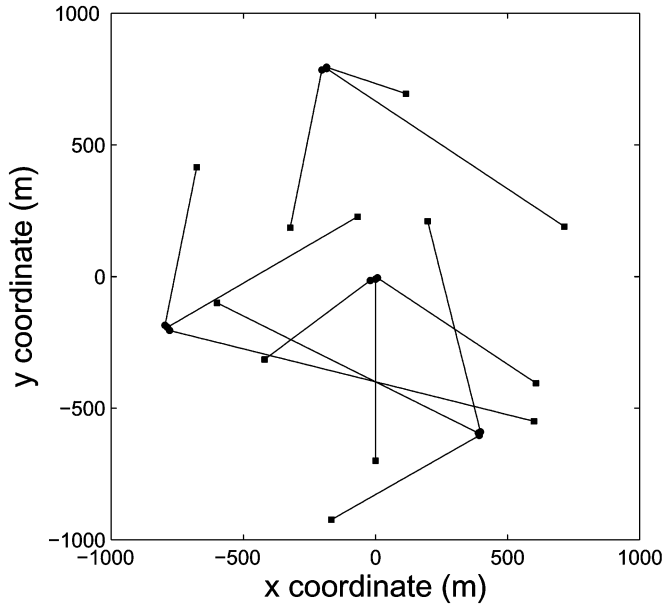


Fig. 1. Target trajectories shown in xy -plane. The start/end points for each track are denoted by \bullet/\blacksquare , respectively.

In all examples, the pruning procedure described in [4] is performed at each time step using a weight threshold of $T = 10^{-5}$, a merging threshold of $U = 4$ m, and a maximum of $J_{\max} = 100$ Gaussian components (see [4] for the meaning of these parameters). The number of targets is estimated using an MAP estimator on the cardinality distribution which is calculated to a maximum of $N_{\max} = 200$ terms.

Two criteria known as the Wasserstein distance (WD) [36] and circular position error probability (CPEP) [37] for a radius of $r = 20$ m are used for performance evaluation. Let \hat{X} and X denote the estimated and true multitarget states, respectively. The WD between \hat{X} and X is defined by

$$d(\hat{X}, X) = \min_{\mathcal{C}} \left[\sum_{i=1}^{|\hat{X}|} \sum_{j=1}^{|X|} C_{ij} \|\hat{x}_i - x_j\|^2 \right]^{1/2}$$

where \mathcal{C} is the set of all transportation matrices (a transportation matrix is one whose entries C_{ij} satisfy $C_{ij} > 0$, $\sum_{i=1}^{|\hat{X}|} C_{ij} = 1/|X|$, and $\sum_{j=1}^{|X|} C_{ij} = 1/|\hat{X}|$). The CPEP is defined by

$$\text{CPEP}(r) = \frac{1}{|\hat{X}|} \sum_{\hat{x} \in \hat{X}} \mathbb{P}\{\|H_k \hat{x} - H_k x\| > r \mid \hat{x} \in \hat{X}\}.$$

Note that the WD penalizes errors in both the estimated state and cardinality, while the CPEP only penalizes errors in individual state estimates but not errors in the estimated cardinality.

1) *Example 1:* Consider a typical tracking scenario in which up to ten targets are present at any time. Target births appear from four different locations according to a Poisson RFS with intensity $\gamma_k(x) = \sum_{i=1}^4 w_{\gamma} \mathcal{N}(x; m_{\gamma}^{(i)}, P_{\gamma})$ where $w_{\gamma} = 0.03$, $m_{\gamma}^{(1)} = [0, 0, 0, 0]^T$, $m_{\gamma}^{(2)} = [400, 0, -600, 0]^T$, $m_{\gamma}^{(3)} = [-800, 0, -200, 0]^T$, $m_{\gamma}^{(4)} = [-200, 0, 800, 0]^T$, and $P_{\gamma} = \text{diag}([10, 10, 10, 10]^T)$. In Fig. 1, the true target trajectories are shown in the xy -plane, while in Fig. 2, the trajectories

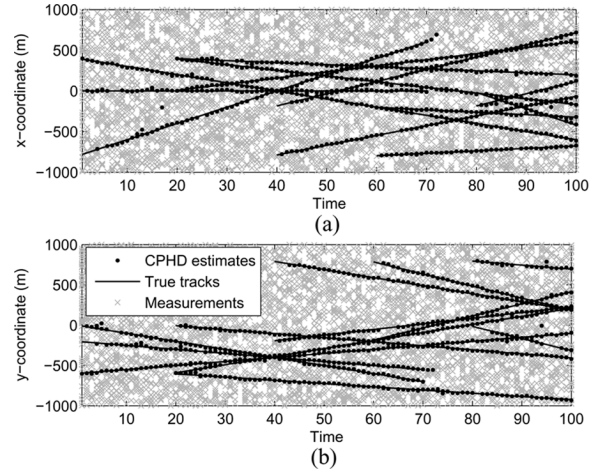


Fig. 2. CPHD filter estimates and true target tracks in x - and y -coordinates versus time.

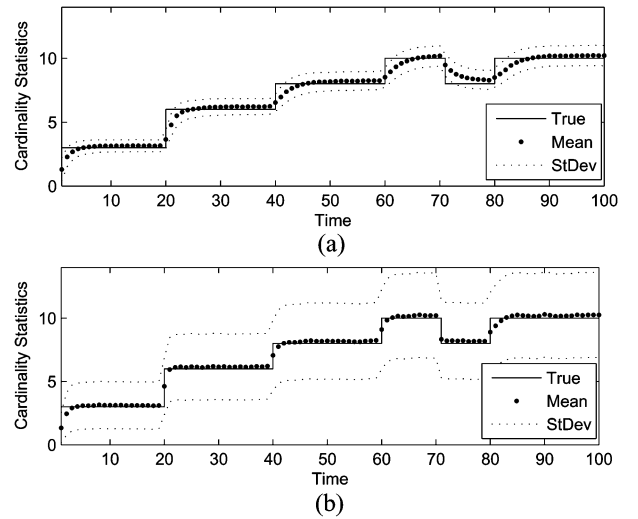


Fig. 3. The 1000 MC run average of cardinality statistics versus time for (a) CPHD and (b) PHD filters.

are shown in x - and y -coordinates versus time with a sample CPHD filter output superimposed. Note that three targets cross at time $k = 40$ while another two cross at time $k = 60$. It can be seen from Fig. 2 that the CPHD filter is able to correctly identify target births, motions, and deaths, and has no trouble handling target crossings. To give an indication of processing time, the Gaussian mixture CPHD filter consumed approximately 10.2 s per sample run over 100 time steps, while the Gaussian mixture PHD filter consumed 2.7 s for the same data (both implemented in MATLAB on a standard notebook computer).

To verify the performance of the proposed Gaussian mixture CPHD filter, 1000 Monte Carlo (MC) runs are performed on the same target trajectories but with independently generated clutter and (target originated) measurements for each trial. For comparison, 1000 MC runs are performed on exactly the same data using the Gaussian mixture PHD filter. In Fig. 3, the true number of targets at each time step is shown along with the MC average of the mean and standard deviation of the cardinality distribution for both the CPHD and PHD filters. The plots demonstrate that both filters converge to the correct number of

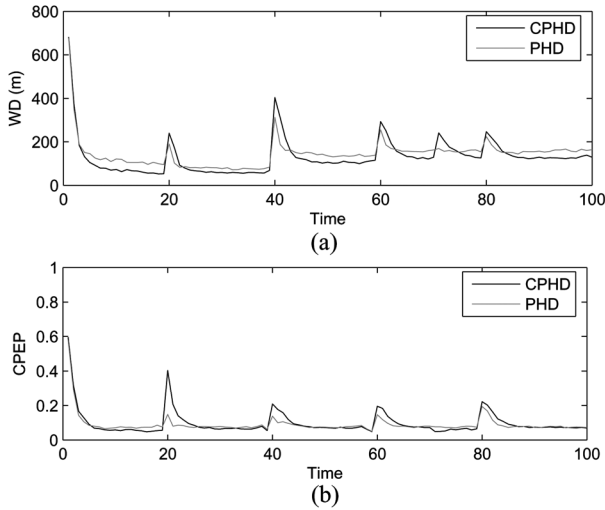


Fig. 4. Comparison of performance measures for PHD/CPHD filters: (a) WD versus time and (b) CPEP (with $r = 20$ m) versus time.

targets present, and that the variance of the cardinality distribution is much smaller in the CPHD filter than in the PHD filter (the average reduction in the variance over 100 time steps is approximately 12.5 times).

Remark: The correct convergence of both the PHD and CPHD filters' mean number of targets is only true as average behavior. More importantly, it is the variance of this estimate that determines the usefulness of the filter since for any given sample path, the PHD filter's estimate of the number of targets is extremely jumpy and inaccurate, whereas the CPHD filter's estimate is far more reliable and accurate.

Further examination of the cardinality statistics reveals a difference in performance regarding the filters' response to changes in the number of targets. Indeed, the simulations also suggest that the average response time of the CPHD filter is slower than that of the PHD filter. A possible explanation for this observation is that the PHD filter's cardinality estimate has a relatively high variance, thus it has low confidence in its estimate and is easily influenced by new incoming measurement information. On the other hand, the CPHD filter's cardinality estimate has a lower variance, and as a consequence, it is much more confident in its estimate and is not easily influenced by new incoming measurements.

For each time step, the MC average of the WD is shown in Fig. 4(a), and the MC average of the CPEP is shown in Fig. 4(b), for both the CPHD and PHD filters. The figure shows that the WD and CPEP exhibit peaks when there is a change in the number of targets. This observation can be expected since the filters are adapting to changes in cardinality at those corresponding time instants. Also note that the peaks in both WD and CPEP curves are smaller in the PHD filter than in the CPHD filter. A possible explanation here is that the PHD filter has a faster response to cardinality changes, and so, on average, incurs a lower penalty in this respect. Also note that during time intervals when the number of targets is steady, the PHD filter has a higher WD value while both filters have similar CPEP values. A possible explanation here is that the CPHD filter produces more accurate state and cardinality estimates in such

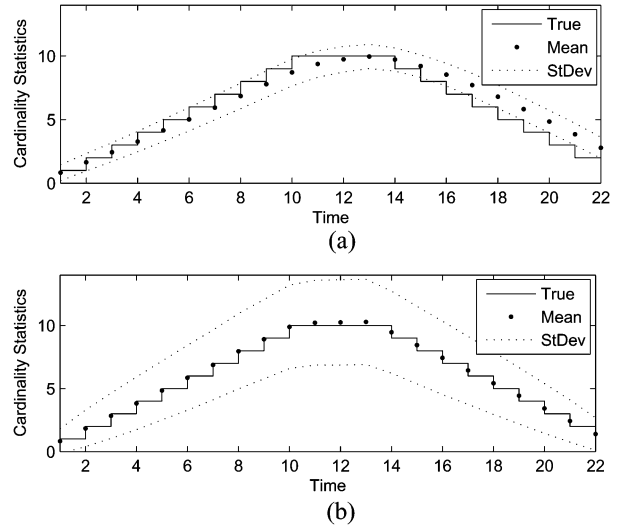


Fig. 5. The 1000 MC run average of cardinality statistics versus time for (a) CPHD and (b) PHD filters.

conditions, and so, on average, incurs a lower WD. On the other hand, while the PHD filter estimates are further away from the true position, many still fall within a surrounding 20-m radius, resulting in roughly the same CPEP.

2) *Example 2:* This example examines the PHD and CPHD filters' responses to rapid changes in the number of targets. For simplicity, a total of ten targets travel along parallel horizontal trajectories, where each trajectory covers a distance of 500 m parallel to the x -axis and is separated at 200-m intervals along the y -axis. For the first half of the simulation, target births occur at consecutive one-unit time intervals, and for the second half, target deaths occur at consecutive one-unit time intervals. Essentially, there is a rapid succession of births to begin, followed by a brief period of having ten targets simultaneously, and a rapid succession of deaths to finish. Target births are modeled on a Poisson RFS with intensity $\gamma_k(x) = \sum_{i=1}^{10} 0.05 \mathcal{N}(x; m_{\gamma}^{(i)}, P_{\gamma})$ where $m_{\gamma}^{(i)} = [-900, 30, -900 + 200(i-1), 0]^T$ and $P_{\gamma} = \text{diag}([5, 15, 5, 15]^T)$. The processing times of the Gaussian mixture CPHD and PHD filters were approximately 2.8 and 1.0 s, respectively, per sample run over 22 time steps (in MATLAB on a standard notebook computer).

As before, 1000 Monte Carlo runs are performed. In Fig. 5, the MC average of the mean and standard deviation of the cardinality distribution are shown versus time for both the CPHD and PHD filters. As expected, the variance of the cardinality distribution is much smaller in the CPHD filter than in the PHD filter. Furthermore, considering the filter response to changes in the number of targets, it appears that the CPHD filter response is delayed by several time instants while the PHD filter response is almost instantaneous. These observations suggest a tradeoff between average response times and reliability of cardinality estimates.

The MC average of the WD and CPEP versus time are shown in Fig. 6(a) and (b), respectively. The plot of the WD shows that the CPHD filter is penalized more than the PHD filter throughout the entire simulation. This is most likely because the number of targets constantly changes causing the CPHD

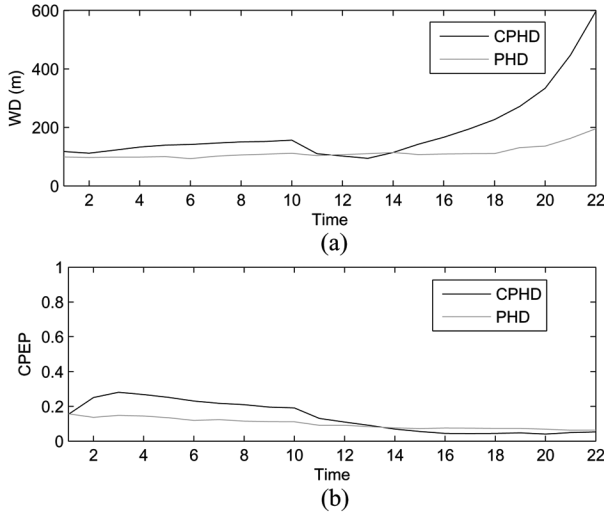


Fig. 6. Comparison of performance measures for PHD/CPHD filters: (a) WD versus time and (b) CPEP (with $r = 20$ m) versus time.

filter to be constantly penalized for errors in its estimated cardinality (having a lagging response to cardinality changes). Note that the plot of the WD for the CPHD filter increases over the second half of the simulation because the lag on the filter increases [as seen in Fig. 5(a)]. If there are no further cardinality changes after $k = 22$ s and the filter is run for several more time steps, the WD values actually drop and settle. The plot of CPEP on the other hand reveals further differences. For the first half of the simulation where there are only target births, the PHD filter appears to perform better. This is most likely because the PHD filter has a fast response to cardinality changes and is able to correctly identify targets births as soon as they appear. For the second half where there are only target deaths, the CPHD appears to perform better. This is most likely a result of the CPHD filter having a slower response to cardinality changes and consequently overestimating the number of targets while not being penalized by the CPEP for doing so.

V. SPECIAL CASE OF THE CPHD FILTER FOR TRACKING A FIXED NUMBER OF TARGETS

In a number of applications, there are neither target births nor deaths and the number of targets is known *a priori* (and fixed), e.g., tracking football players on a field during playing time. While the CPHD filter is applicable in this case, it is more efficient to exploit the explicit knowledge of the number of targets. This section presents a special case of the CPHD recursion for tracking a fixed number of targets in clutter and proposes a closed-form implementation for linear Gaussian multitarget models.

A. Recursion

Since there are no births or deaths, the birth intensity is $\gamma_k(x) = 0$ and the probability of survival is $p_{S,k}(x) = 1$. Let $N \in \mathbb{N}$ be the fixed and known number of targets. Then, it follows from the CPHD cardinality recursion (9) and (12) that the cardinality distribution at any time must be a Dirac delta

function centered on N , i.e., $p_{k|k-1}(\cdot) = p_k(\cdot) = \delta_N(\cdot)$. Moreover, it can be seen that the predicted and updated intensities (10) and (13) reduce to

$$v_{k|k-1}(x) = \int f_{k|k-1}(x|\zeta) v_{k-1}(\zeta) d\zeta \quad (42)$$

$$v_k(x) = \frac{\Upsilon_k^1[v_{k|k-1}, Z_k](N)}{\Upsilon_k^0[v_{k|k-1}, Z_k](N)} [1 - p_{D,k}(x)] v_{k|k-1}(x) + \sum_{z \in Z_k} \frac{\Upsilon_k^1[v_{k|k-1}, Z_k \setminus \{z\}](N)}{\Upsilon_k^0[v_{k|k-1}, Z_k](N)} \times \psi_{k,z}(x) v_{k|k-1}(x) \quad (43)$$

where $\Upsilon_k^u[v, Z](\cdot)$ is given in (14).

Equations (42) and (43) define a special case of the CPHD recursion for tracking a fixed number of targets in clutter (including the case of a single target). The previous recursion also admits a closed-form solution under linear Gaussian assumptions as stated in Section VI.

B. Closed-Form Recursion

A closed-form solution for CPHD recursion was established for the special class of linear Gaussian multitarget models in Section III-B. Since the recursion (42) and (43) for tracking a fixed number of targets in clutter is a special case of the CPHD recursion, it also admits a closed-form solution for the class of linear Gaussian multitarget models. Corollaries 1 and 2 follow directly from Propositions 3 and 4 and establish an analytic propagation of the posterior intensity given by the recursion (42) and (43).

Corollary 1: Suppose at time $k-1$ that the posterior intensity v_{k-1} is a Gaussian mixture of the form (22). Then, the predicted intensity at time k is also a Gaussian mixture and is given by $v_{k|k-1}(x) = v_{S,k|k-1}(x)$ where $v_{S,k|k-1}(\cdot)$ is given by (25).

Corollary 2: Suppose at time k that the predicted intensity $v_{k|k-1}$ is a Gaussian mixture of the form (28). Then, the posterior intensity at time k is also a Gaussian mixture and is given by

$$v_k(x) = \frac{\Psi_k^1[w_{k|k-1}, Z_k](N)}{\Psi_k^0[w_{k|k-1}, Z_k](N)} (1 - p_{D,k}) v_{k|k-1}(x) + \sum_{z \in Z_k} \sum_{j=1}^{J_{k|k-1}} w_k^{(j)}(z) \mathcal{N}(x; m_k^{(j)}(z), P_k^{(j)}) \quad (44)$$

where

$$w_k^{(j)}(z) = p_{D,k} w_{k|k-1}^{(j)}(z) q_k^{(j)}(z) \frac{\Psi_k^1[w_{k|k-1}, Z_k \setminus \{z\}](N)}{\Psi_k^0[w_{k|k-1}, Z_k](N)} \frac{\langle 1, \kappa_k \rangle}{\kappa_k(z)} \quad (45)$$

$\Psi_k^u[w, Z](\cdot)$ is given by (31), (32), and (34); $w_{k|k-1}$ is given by (33); $q_k^{(j)}(z)$ is given by (35); $m_k^{(j)}(z)$ is given by (39); and $P_k^{(j)}$ is given by (40) and (41).

C. Demonstrations and Comparison with JPDA

We examine the performance of the special case CPHD filter for tracking a fixed number of targets by benchmarking with the JPDA filter. Note that while the JPDA filter assumes a known and fixed number of targets, the general CPHD filter does not. For this reason, a direct comparison between the CPHD and

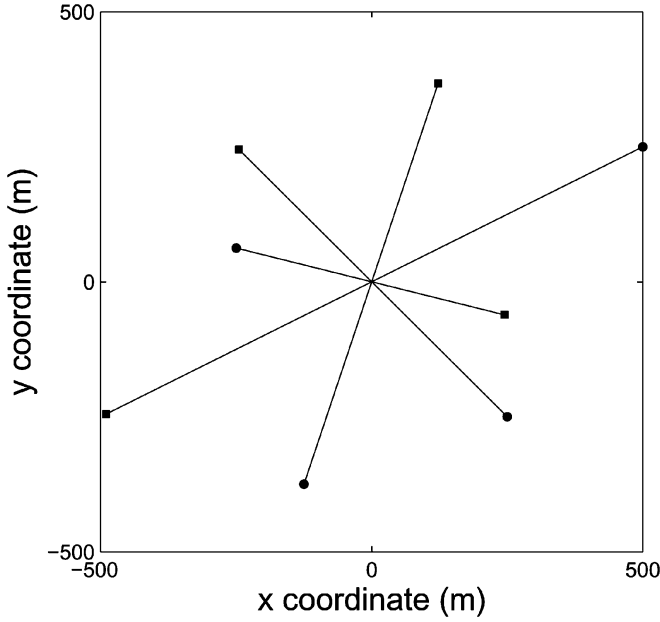


Fig. 7. True target tracks in the xy -plane. The start/end points for each track are denoted by \bullet/\blacksquare , respectively.

JPDA filters is normally not a fair assessment. However, using the special case of the CPHD filter proposed here, a direct comparison with the JPDA filter is fair since both filters use the same prior knowledge. Note that in terms of complexity, the CPHD filter is linear in the number of targets and cubic in the number of measurements, while the standard JPDA filter is an NP-hard formulation [38].

In this demonstration, there is a total of 100 time steps and exactly four targets which all cross paths at time $k = 50$. The true target tracks are shown in Fig. 7. Each target moves with a fixed velocity according to the motion and measurement model given in Section IV. For the CPHD filter, pruning and merging of mixture components is performed using a weight threshold of $T = 10^{-3}$, a merging threshold of $U = 15$ m, and a maximum of $J_{\max} = 100$ Gaussian components (see [4] for the meaning of these parameters). Per scan of data, the throughput time for the CPHD filter is typically around 0.05 s, while the throughput time for the standard JPDA filter is several orders of magnitude larger (implemented in MATLAB on a standard notebook computer). It can be seen that performing MC runs for the standard JPDA filter would require an inordinate amount of time. Hence, for the purposes of comparison, the JPDA filter is run with measurement gating using a 99% validation region around each individual target so that its typical throughput time is the same order of magnitude as that of the CPHD filter.

To compare the performance of the Gaussian mixture CPHD filter and the JPDA filter, 1000 MC runs are performed for both filters over varying clutter rates and detection probabilities. First, the average clutter intensity λ_c is varied from 0 m^{-2} to $2.5 \times 10^{-5} \text{ m}^{-2}$ while the probability of target detection remains unchanged at $p_{D,k} = 0.98$. The time-averaged WD and time-averaged CPEP are shown versus the clutter rate in Fig. 8. Second, the detection probability $p_{D,k}$ is varied from 0.7 to 1.0 while the average clutter rate is fixed at $\lambda_c = 1.25 \times 10^{-5} \text{ m}^{-2}$.

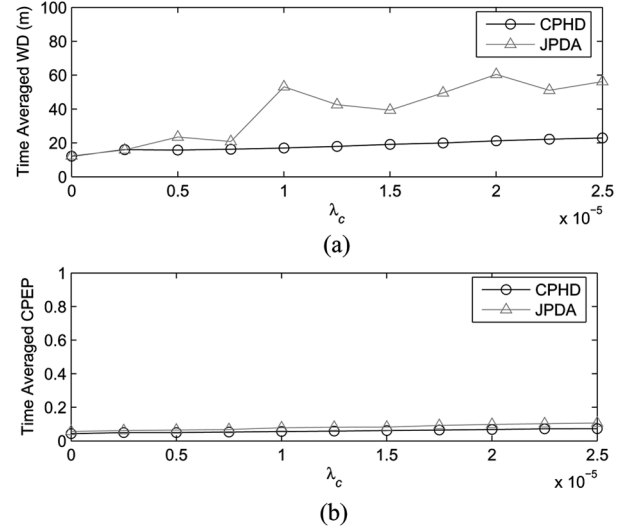


Fig. 8. Tracking performance for varying λ_c ($p_{D,k} = 0.98$ is fixed; CPEP radius $r = 20$ m).

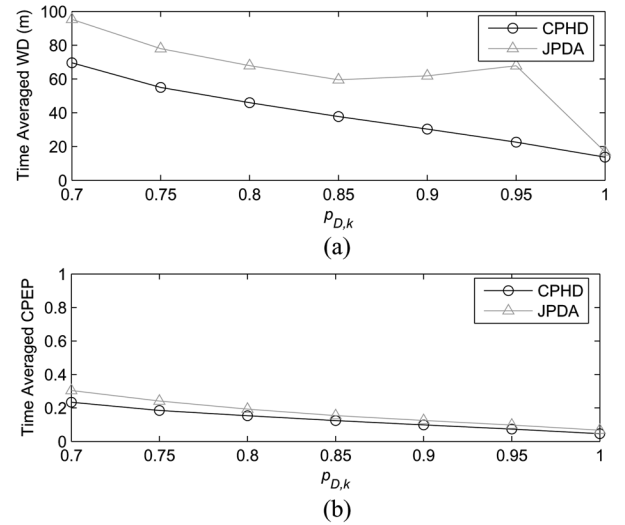


Fig. 9. Tracking performance for varying $p_{D,k}$ ($\lambda_c = 1.25 \times 10^{-5} \text{ m}^{-2}$ is fixed; CPEP radius $r = 20$ m).

The time-averaged WD and time-averaged CPEP are shown versus the probability of detection in Fig. 9.

These results suggest (at least in this particular scenario) that there is a definite performance advantage favoring the Gaussian mixture CPHD filter over the standard JPDA filter. For high rates of clutter and low probability of detection, the observed performance difference is noticeable; however, for high SNR, the observed performance difference tends to be smaller. These observations are most likely caused by the JPDA filter having difficulty resolving target crossings, whereas the CPHD filter is less adversely affected by target crossings owing to its propagation of the complete posterior intensity.

VI. EXTENSION TO NONLINEAR MODELS

In this section, two nonlinear extensions of the Gaussian mixture CPHD recursion are proposed using linearization and unscented transforms, analogous to the approach in [4] for ex-

tending the Gaussian mixture PHD filter. In essence, the assumptions on the form of the single-target dynamical and measurement model given by the transition density $f_{k|k-1}(\cdot|\cdot)$ and the likelihood $g_k(\cdot|\cdot)$ are relaxed to the nonlinear functions in the state and noise variables

$$\begin{aligned} x_k &= \varphi_k(x_{k-1}, \nu_{k-1}) \\ z_k &= h_k(x_k, \varepsilon_k) \end{aligned}$$

where φ_k and h_k are the nonlinear state and measurement functions, respectively, and ν_{k-1} and ε_k are independent zero-mean Gaussian noise processes with covariance matrices Q_{k-1} and R_k , respectively.

A. Extended Kalman CPHD (EK-CPHD) Recursion

Analogous to the extended Kalman filter (EKF) [39], [40], a nonlinear approximation to the Gaussian mixture CPHD recursion is proposed based on applying local linearizations of φ_k and h_k as follows.

In Proposition 3, the prediction step can be made to approximate nonlinear target motions by predicting the mixture components of surviving targets using first-order approximations wherever nonlinearities are encountered, i.e., by using the approximations (46) and (47) given in place of the originals (26) and (27)

$$m_{k|k-1}^{(j)} = \varphi_k \left(m_{k-1}^{(j)}, 0 \right) \quad (46)$$

$$P_{k|k-1}^{(j)} = G_{k-1}^{(j)} Q_{k-1} \left[G_{k-1}^{(j)} \right]^T + F_{k-1}^{(j)} P_{k-1}^{(j)} \left[F_{k-1}^{(j)} \right]^T \quad (47)$$

where

$$F_{k-1}^{(j)} = \left. \frac{\partial \varphi_k(x, 0)}{\partial x} \right|_{x=m_{k-1}^{(j)}} \quad G_{k-1}^{(j)} = \left. \frac{\partial \varphi_k(m_{k-1}^{(j)}, \nu)}{\partial \nu} \right|_{\nu=0} \quad (48)$$

In Proposition 4, the update step can be made to approximate nonlinear measurement models by updating the each of the predicted mixture components using first-order approximations wherever nonlinearities are encountered, i.e., by using the approximations (49) and (50) given in place of the originals (36) and (37) and using the linearizations in (51) for the calculation of (40) and (41)

$$\eta_{k|k-1}^{(j)} = h_k \left(m_{k|k-1}^{(j)}, 0 \right) \quad (49)$$

$$S_k^{(j)} = U_k^{(j)} R_k \left[U_k^{(j)} \right]^T + H_k^{(j)} P_{k|k-1}^{(j)} \left[H_k^{(j)} \right]^T \quad (50)$$

where

$$H_k^{(j)} = \left. \frac{\partial h_k(x, 0)}{\partial x} \right|_{x=m_{k|k-1}^{(j)}} \quad U_k^{(j)} = \left. \frac{\partial h_k(m_{k|k-1}^{(j)}, \varepsilon)}{\partial \varepsilon} \right|_{\varepsilon=0} \quad (51)$$

B. Unscented Kalman CPHD (UK-CPHD) Recursion

Analogous to the unscented Kalman filter (UKF) [41], a nonlinear approximation to the Gaussian mixture CPHD recursion is proposed based on the unscented transform (UT). The strategy

here is to use the UT to propagate the first and second moments of each mixture component through the nonlinear transformations φ_k and h_k as follows.

To begin, for each mixture component of the posterior intensity, using the UT with mean $\mu_k^{(j)}$ and covariance $C_k^{(j)}$, generate a set of sigma points $\{y_k^{(\ell)}\}_{\ell=0}^L$ and weights $\{u^{(\ell)}\}_{\ell=0}^L$ where

$$\begin{aligned} \mu_k^{(j)} &= [m_{k-1}^{(j)} \quad 0^T \quad 0^T]^T \\ C_k^{(j)} &= \text{diag} \left(P_{k-1}^{(j)}, Q_{k-1}, R_k \right). \end{aligned}$$

Then, partition the sigma points into

$$y_k^{(\ell)} = \left[\left(x_{k-1}^{(\ell)} \right)^T, \left(\nu_{k-1}^{(\ell)} \right)^T, \left(\varepsilon_k^{(\ell)} \right)^T \right]^T$$

for $\ell = 0, \dots, L$ and proceed as follows.

For the prediction, the sigma points are propagated through the transition function according to $x_{k|k-1}^{(\ell)} = \varphi_k \left(x_{k-1}^{(\ell)}, \nu_{k-1}^{(\ell)} \right)$ for $\ell = 0, \dots, L$. Then, in Proposition 3, the prediction step can be made to approximate nonlinear target motions by using the approximations (52) and (53) given in place of the originals (26) and (27)

$$m_{k|k-1}^{(j)} = \sum_{\ell=0}^L u^{(\ell)} x_{k|k-1}^{(\ell)} \quad (52)$$

$$P_{k|k-1}^{(j)} = \sum_{\ell=0}^L u^{(\ell)} \left(x_{k|k-1}^{(\ell)} - m_{k|k-1}^{(j)} \right) \left(x_{k|k-1}^{(\ell)} - m_{k|k-1}^{(j)} \right)^T \quad (53)$$

For the update, the sigma points are propagated through the measurement function according to $z_{k|k-1}^{(\ell)} = h_k \left(x_{k|k-1}^{(\ell)}, \varepsilon_k^{(\ell)} \right)$ for $\ell = 0, \dots, L$. Then, in Proposition 4, the update step can be made to approximate nonlinear measurement models by using the approximations (54) and (55) given in place of the originals (36) and (37), and using (56) and (57) given in place of the originals (40) and (41)

$$\eta_{k|k-1}^{(i)} = \sum_{\ell=0}^L u^{(\ell)} z_{k|k-1}^{(\ell)} \quad (54)$$

$$S_k^{(i)} = \sum_{\ell=0}^L u^{(\ell)} \left(z_{k|k-1}^{(\ell)} - \eta_{k|k-1}^{(i)} \right) \left(z_{k|k-1}^{(\ell)} - \eta_{k|k-1}^{(i)} \right)^T \quad (55)$$

$$P_k^{(i)} = P_{k|k-1}^{(i)} - G_k^{(i)} \left[S_k^{(i)} \right]^{-1} \left[G_k^{(i)} \right]^T \quad (56)$$

$$K_k^{(i)} = G_k^{(i)} \left[S_k^{(i)} \right]^{-1} \quad (57)$$

$$G_k^{(i)} = \sum_{\ell=0}^L u^{(\ell)} \left(x_{k|k-1}^{(\ell)} - m_{k|k-1}^{(i)} \right) \left(z_{k|k-1}^{(\ell)} - m_{k|k-1}^{(i)} \right)^T \quad (58)$$

Notice that the EK-CPHD and UK-CPHD recursions have similar advantages and disadvantages to their single-target counterparts. In particular, the EK-CPHD recursion requires the calculation of Jacobians, and hence, is only applicable when the state and measurement models are differentiable. In

contrast, the UK-CPHD recursion completely avoids the differentiation requirement and is even applicable to models with discontinuities. Finally, note that the EK-CPHD and UK-CPHD approximations are much less computationally expensive than SMC approximations in dealing with nonlinearities, and that state estimates can still be extracted very easily due to the underlying Gaussian mixture implementation.

Remark: The nonlinear EK-CPHD and UK-CPHD filter approximations apply directly to the Gaussian mixture implementation of the special case CPHD filter for tracking a fixed number of targets in clutter.

C. Nonlinear Demonstrations

This section presents a nonlinear tracking scenario in order to demonstrate the performance of the Gaussian mixture EK-CPHD and UK-CPHD filters. Here, a nearly constant turn model with varying turn rate [42] together with bearing and range measurements is considered. The observation region is the half disc of radius 2000 m. For clarity, only five targets appear over the course of the simulation in which there are various births and deaths. The target state variable $x_k = [\tilde{x}_k^T, \omega_k]^T$ comprises the planar position and velocity $\tilde{x}_k^T = [p_{x,k}, \dot{p}_{x,k}, p_{y,k}, \dot{p}_{y,k}]^T$ as well as the turn rate ω_k . The state transition model is

$$\tilde{x}_k = F(\omega_{k-1})\tilde{x}_{k-1} + Gw_{k-1} \quad (59)$$

$$\omega_k = \omega_{k-1} + \Delta u_{k-1} \quad (60)$$

where

$$F(\omega) = \begin{bmatrix} 1 & \frac{\sin \omega \Delta}{\omega} & 0 & -\frac{1 - \cos \omega \Delta}{\omega} \\ 0 & \cos \omega \Delta & 0 & -\sin \omega \Delta \\ 0 & \frac{1 - \cos \omega \Delta}{\omega} & 1 & \frac{\sin \omega \Delta}{\omega} \\ 0 & \sin \omega \Delta & 0 & \cos \omega \Delta \end{bmatrix}$$

$$G = \begin{bmatrix} \frac{\Delta^2}{2} & 0 \\ \frac{\Delta^2}{2} & 0 \\ 0 & \frac{\Delta^2}{2} \\ 0 & \frac{\Delta^2}{2} \end{bmatrix}$$

$w_{k-1} \sim \mathcal{N}(\cdot; 0, \sigma_w^2 I)$ and $u_{k-1} \sim \mathcal{N}(\cdot; 0, \sigma_u^2 I)$ with $\Delta = 1$ s, $\sigma_w = 15$ m/s², and $\sigma_u = \pi/180$ rad/s. The sensor observation is a noisy bearing and range vector given by

$$z_k = \begin{bmatrix} \arctan\left(\frac{p_{y,k}}{p_{x,k}}\right) \\ \sqrt{p_{x,k}^2 + p_{y,k}^2} \end{bmatrix} + \varepsilon_k \quad (61)$$

where $\varepsilon_k \sim \mathcal{N}(\cdot; 0, R_k)$ with $R_k = \text{diag}([\sigma_\theta^2, \sigma_r^2]^T)$, $\sigma_\theta = 2(\pi/180)$ rad, and $\sigma_r = 10$ m. The birth process follows a Poisson RFS with intensity $\gamma_k(x) = 0.1\mathcal{N}(x; m_\gamma^{(1)}, P_\gamma) + 0.1\mathcal{N}(x; m_\gamma^{(2)}, P_\gamma)$, where $m_\gamma^{(1)} = [-1000, 0, -500, 0]^T$, $m_\gamma^{(2)} = [1050, 0, 1070, 0]^T$, and $P_\gamma = \text{diag}([50, 50, 50, 50, 6(\pi/180)]^T)$. The probability of target survival and detection are $p_{S,k} = 0.99$ and $p_{D,k} = 0.98$, respectively. Clutter follows a Poisson RFS with intensity $\lambda_c = 3.2 \times 10^{-3}$ (rad m)⁻¹ over the region

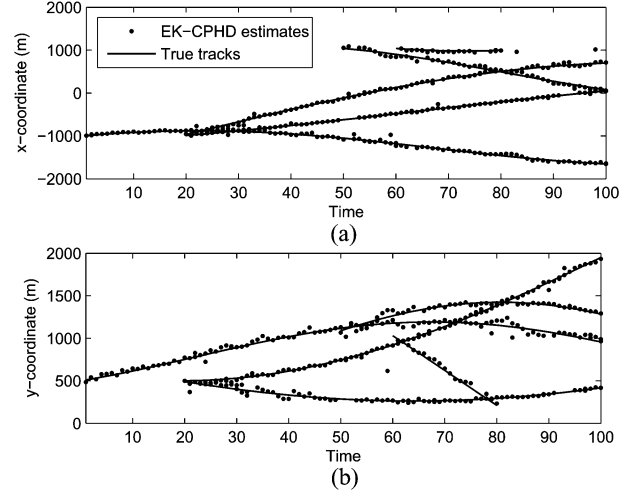


Fig. 10. True tracks and EK-CPHD filter estimates.

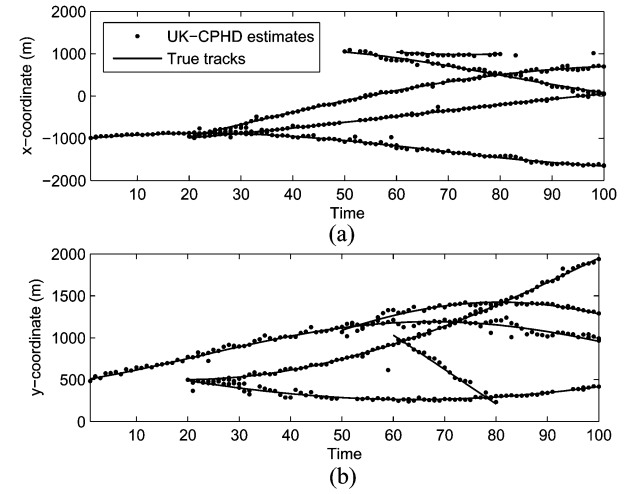


Fig. 11. True tracks and UK-CPHD filter estimates.

$[-\pi/2, \pi/2]$ rad $\times [0, 2000]$ m (hence, the average number of false detections per frame is 20).

For both the EK-CPHD and UK-CPHD filters, pruning and merging of mixture components is performed as described in Section IV, while the number of targets is estimated with an MAP estimator on the cardinality distribution which is calculated to $N_{\max} = 200$ terms.

Both the EK-CPHD and UK-CPHD filters are run on the same measurement data. The true trajectories and a sample filter output for the EK-CPHD and UK-CPHD are shown in Figs. 10 and 11, respectively. It can be seen that the both EK and UK approximation to the Gaussian mixture CPHD filter are able to identify all target births and track the nonlinear motion well. Notice also that the filters have no trouble estimating the states of the two targets which cross paths at time $k = 80$.

VII. CONCLUSION

This paper proposed a Gaussian mixture implementation of the CPHD filter as a solution to the multitarget detection and estimation problem. It was shown that for the class of linear Gaussian multitarget models, the CPHD recursion admits a

closed-form solution. In particular, closed-form expressions for propagating the Gaussian mixture intensity, as well as for the cardinality distribution were derived. Furthermore, efficient techniques for propagating the intensity and cardinality distribution were given. A special case of the CPHD filter for tracking a fixed number of targets was proposed, along with a closed-form recursion for linear Gaussian multitarget models. Extensions to nonlinear models were provided via linearization and unscented transform techniques. Simulations verified that the proposed Gaussian mixture CPHD filter performs accurately and shows a dramatic reduction in the variance of the estimated number of targets when compared to the Gaussian mixture PHD filter. Moreover, interesting differences in the CPHD and PHD filters' response to changes in the number of targets were observed. Additionally, simulations suggested that the special case CPHD filter for tracking a fixed number of targets has a noticeable performance advantage compared to the standard JPDA filter. The complexity of the CPHD filter is linear in the number of targets and cubic in the number of measurements, while the standard JPDA filter is an NP-hard formulation. Finally, simulations showed that the proposed extensions to nonlinear models are suitable algorithms for problems involving mild nonlinearities.

APPENDIX

Here, we derive the CPHD recursion given in Section III from the original recursion proposed in [24] and [25]. Recall that $v_{k|k-1}$ and v_k denote the predicted and posterior intensities respectively. Following [24] and [25], let $G_{k|k-1}$ and G_k denote the probability generating functions of $p_{k|k-1}$ and p_k , respectively; $G_{\Gamma,k}$ and $G_{K,k}$ denote the probability generating functions of $p_{\Gamma,k}$ and $p_{K,k}$, respectively; $G^{(i)}(\cdot)$ denote the i th derivative of $G(\cdot)$ and $\hat{G}^{(i)}(\cdot) = G^{(i)}(\cdot)/G^{(1)}(1)^i$; $c_k(z) = \kappa_k(z)/\langle 1, \kappa_k \rangle$ denote the density of clutter measurements; $q_{D,k} = 1 - p_{D,k}$ denote the missed detection probability; and $\sigma_j(Z)$ denote $e_j(\Xi_k(v_{k|k-1}, Z))$. Also, let $\bar{v} = v/\langle 1, v \rangle$ for any unnormalized density v .

Proof of Proposition 1: Consider the original CPHD prediction as given in [24] and [25]

$$v_{k|k-1}(x) = \int p_{S,k}(\zeta) f_{k|k-1}(x|\zeta) v_{k-1}(\zeta) d\zeta + \gamma_k(x) \quad (\text{A.1})$$

$$p_{k|k-1}(n) = \sum_{j=0}^n p_{\Gamma,k}(n-j) \times \left[\frac{1}{j!} G_{k-1}^{(j)}(1 - \langle p_{S,k}, \bar{v}_{k-1} \rangle) \langle p_{S,k}, \bar{v}_{k-1} \rangle^j \right]. \quad (\text{A.2})$$

Note that the intensity prediction (A.1) and (10) are identical. To simplify the cardinality prediction (A.2), using $\bar{v}_{k-1} = v_{k-1}/\langle 1, v_{k-1} \rangle$ and $G_{k-1}^{(j)}(y) = \sum_{\ell=j}^{\infty} P_j^\ell p_{k-1}(\ell) y^{\ell-j}$, the bracketed expression in (A.2) simplifies to

$$\begin{aligned} & \frac{1}{j!} \sum_{\ell=j}^{\infty} P_j^\ell \cdot p_{k-1}(\ell) \left[1 - \frac{\langle p_{S,k}, v_{k-1} \rangle}{\langle 1, v_{k-1} \rangle} \right]^{\ell-j} \left[\frac{\langle p_{S,k}, v_{k-1} \rangle}{\langle 1, v_{k-1} \rangle} \right]^j \\ &= \sum_{\ell=j}^{\infty} \frac{P_j^\ell}{j!} p_{k-1}(\ell) \left[\frac{\langle p_{S,k}, v_{k-1} \rangle}{\langle 1, v_{k-1} \rangle} \right]^j \\ & \quad \times \left[1 - \frac{\langle p_{S,k}, v_{k-1} \rangle}{\langle 1, v_{k-1} \rangle} \right]^{\ell-j} \left[\frac{\langle 1, v_{k-1} \rangle}{\langle 1, v_{k-1} \rangle} \right]^{\ell-j} \\ &= \sum_{\ell=j}^{\infty} C_j^\ell \cdot \frac{\langle p_{S,k}, v_{k-1} \rangle^j \langle 1 - p_{S,k}, v_{k-1} \rangle^{\ell-j}}{\langle 1, v_{k-1} \rangle^\ell} p_{k-1}(\ell) \\ &= \Pi_{k|k-1}[v_{k-1}, p_{k-1}](j). \end{aligned} \quad (\text{A.3})$$

Hence, substituting (A.3) into (A.2), we obtain the CPHD cardinality prediction (9) as required.

Proof of Proposition 2: Consider now the original CPHD update (see [24] and [25]) as given in (A.4) and (A.5) shown at the bottom of the page.

$$\begin{aligned} v_k(x) = q_{D,k}(x) & \left[\frac{\sum_{j=0}^{|Z_k|} G_{K,k}^{(|Z_k|-j)}(0) \cdot \hat{G}_{k|k-1}^{(j+1)}(\langle q_{D,k}, \bar{v}_{k|k-1} \rangle) \cdot \sigma_j(Z_k)}{\sum_{i=0}^{|Z_k|} G_{K,k}^{(|Z_k|-i)}(0) \cdot \hat{G}_{k|k-1}^{(i)}(\langle q_{D,k}, \bar{v}_{k|k-1} \rangle) \cdot \sigma_i(Z_k)} \right] v_{k|k-1}(x) \\ & + p_{D,k}(x) \sum_{z \in Z_k} \frac{g_k(z|x)}{c_k(z)} \left[\frac{\sum_{j=0}^{|Z_k|-1} G_{K,k}^{(|Z_k|-j-1)}(0) \cdot \hat{G}_{k|k-1}^{(j+1)}(\langle q_{D,k}, \bar{v}_{k|k-1} \rangle) \cdot \sigma_j(Z_k \setminus \{z\})}{\sum_{i=0}^{|Z_k|} G_{K,k}^{(|Z_k|-i)}(0) \cdot \hat{G}_{k|k-1}^{(i)}(\langle q_{D,k}, \bar{v}_{k|k-1} \rangle) \cdot \sigma_i(Z_k)} \right] v_{k|k-1}(x) \quad (\text{A.4}) \end{aligned}$$

$$p_k(n) = \frac{\sum_{j=0}^{|Z_k|} G_{K,k}^{(|Z_k|-j)}(0) \cdot \frac{1}{(n-j)!} \hat{G}_{k|k-1}^{(j)(n-j)}(0) \cdot \langle q_{D,k}, \bar{v}_{k|k-1} \rangle^{n-j} \sigma_j(Z_k)}{\sum_{i=0}^{|Z_k|} G_{K,k}^{(|Z_k|-i)}(0) \cdot \hat{G}_{k|k-1}^{(i)}(\langle q_{D,k}, \bar{v}_{k|k-1} \rangle) \cdot \sigma_i(Z_k)}. \quad (\text{A.5})$$

We first simplify the intensity update (A.4). Note that both the numerator and denominator of the two bracketed terms in (A.4) are all of the general form

$$\sum_{j=0}^{|Z|} G_{K,k}^{(|Z|-j)}(0) \cdot \hat{G}_{k|k-1}^{(j+u)}(\langle q_{D,k}, \bar{v}_{k|k-1} \rangle) \cdot \sigma_j(Z). \quad (\text{A.6})$$

Using $\bar{v}_{k|k-1} = v_{k|k-1} / \langle 1, v_{k|k-1} \rangle$, $G_{K,k}^{(i)}(0) = i! p_{K,k}(i)$, $\hat{G}_{k|k-1}^{(i)}(y) = \langle 1, v_{k|k-1} \rangle^{-i} \sum_{n=i}^{\infty} P_i^n \cdot p_{k|k-1}(n) \cdot y^{n-i}$, and $P_i^n = 0$ for all integers $n < i$, it can be seen that (A.6) simplifies to

$$\begin{aligned} & \sum_{j=0}^{|Z|} (|Z| - j)! p_{K,k}(|Z| - j) \frac{1}{\langle 1, v_{k|k-1} \rangle^{j+u}} \\ & \times \sum_{n=j+u}^{\infty} P_{j+u}^n p_{k|k-1}(n) \frac{\langle q_{D,k}, v_{k|k-1} \rangle^{n-(j+u)}}{\langle 1, v_{k|k-1} \rangle^{n-(j+u)}} \sigma_j(Z) \\ & = \sum_{j=0}^{|Z|} (|Z| - j)! p_{K,k}(|Z| - j) \sum_{n=j+u}^{\infty} P_{j+u}^n p_{k|k-1}(n) \\ & \times \frac{\langle q_{D,k}, v_{k|k-1} \rangle^{n-(j+u)}}{\langle 1, v_{k|k-1} \rangle^n} \sigma_j(Z) \\ & = \sum_{j=0}^{\min(|Z|, n)} (|Z| - j)! p_{K,k}(|Z| - j) \sum_{n=0}^{\infty} P_{j+u}^n p_{k|k-1}(n) \\ & \times \frac{\langle q_{D,k}, v_{k|k-1} \rangle^{n-(j+u)}}{\langle 1, v_{k|k-1} \rangle^n} \sigma_j(Z) \\ & = \sum_{n=0}^{\infty} p_{k|k-1}(n) \left[\sum_{j=0}^{\min(|Z|, n)} (|Z| - j)! p_{K,k}(|Z| - j) \right. \\ & \quad \left. \times P_{j+u}^n \frac{\langle q_{D,k}, v_{k|k-1} \rangle^{n-(j+u)}}{\langle 1, v_{k|k-1} \rangle^n} \sigma_j(Z) \right]. \end{aligned}$$

Since the bracketed expression in the last line of previous equation is precisely the definition of $\Upsilon_k^u[v_{k|k-1}, Z](n)$, it follows that (A.6) can be written as

$$\sum_{n=0}^{\infty} p_{k|k-1}(n) \Upsilon_k^u[v_{k|k-1}, Z](n) = \langle p_{k|k-1}, \Upsilon_k^u[v_{k|k-1}, Z] \rangle. \quad (\text{A.7})$$

Substituting into (A.7), $Z = Z_k \setminus \{z\}$ and $u = 1$ yields the numerator of the first bracketed term in (A.4); $Z = Z_k$ and $u = 1$ yields the numerator of the second bracketed term in (A.4); $Z = Z_k$ and $u = 0$ yields the denominator of the both bracketed terms in (A.4). Thus, we have established the CPHD intensity update (13) as required.

Now, we simplify the cardinality update (A.5). The numerator in (A.5) can be simplified using $G_{K,k}^{(i)}(0) = i! p_{K,k}(i)$ and $\hat{G}_{k|k-1}^{(j)(n-j)}(0) = \langle 1, v_{k|k-1} \rangle^{-j} n! p_{k|k-1}(n)$ as follows:

$$\begin{aligned} & \sum_{j=0}^{|Z|} \frac{G_{K,k}^{(|Z|-j)}(0)}{(n-j)!} \hat{G}_{k|k-1}^{(j)(n-j)}(0) \langle q_{D,k}, \bar{v}_{k|k-1} \rangle^{n-j} \sigma_j(Z_k) \\ & = \sum_{j=0}^{|Z|} \frac{(|Z| - j)! p_{K,k}(|Z| - j)}{(n-j)!} \\ & \times \frac{n! p_{k|k-1}(n)}{\langle 1, v_{k|k-1} \rangle^j} \frac{\langle q_{D,k}, v_{k|k-1} \rangle^{n-j}}{\langle 1, v_{k|k-1} \rangle^{n-j}} \sigma_j(Z_k) \\ & = \sum_{j=0}^{|Z|} (|Z| - j)! p_{K,k}(|Z| - j) P_j^n \\ & \times \frac{\langle q_{D,k}, v_{k|k-1} \rangle^{n-j}}{\langle 1, v_{k|k-1} \rangle^n} \sigma_j(Z) p_{k|k-1}(n) \\ & = \Upsilon_k^0[v_{k|k-1}, Z](n) p_{k|k-1}(n). \end{aligned}$$

Furthermore, since the denominator in (A.5) is of the form (A.7), we have established the CPHD cardinality update (12) as required.

ACKNOWLEDGMENT

The authors would like thank Dr. R. Mahler for his valuable discussions and feedback.

REFERENCES

- [1] I. Goodman, R. Mahler, and H. Nguyen, *Mathematics of Data Fusion*. Norwell, MA: Kluwer, 1997.
- [2] R. Mahler, "Multitarget Bayes filtering via first-order multitarget moments," *IEEE Trans. Aerosp. Electron. Syst.*, vol. 39, no. 4, pp. 1152–1178, Oct. 2003.
- [3] B. Vo, S. Singh, and A. Doucet, "Sequential Monte Carlo methods for multitarget filtering with random finite sets," *IEEE Trans. Aerosp. Electron. Syst.*, vol. 41, no. 4, pp. 1224–1245, Oct. 2005.
- [4] B. Vo and W. Ma, "The Gaussian mixture probability hypothesis density filter," *IEEE Trans. Signal Process.*, vol. 54, no. 11, pp. 4091–4104, Nov. 2006.
- [5] H. Sidenbladh, "multitarget particle filtering for the probability hypothesis density," in *Proc. Int. Conf. Inf. Fusion*, Cairns, Australia, 2003, pp. 800–806.
- [6] T. Zajic, R. Ravichandran, R. Mahler, R. Mehra, and M. Noviskey, "Joint tracking and identification with robustness against unmodeled targets," *SPIE Proc. Signal Process., Sensor Fusion Target Recognit. XII*, vol. 5096, pp. 279–290, 2003.
- [7] N. Ikoma, T. Uchino, and H. Maeda, "Tracking of feature points in image sequence by SMC implementation of the PHD filter," in *Proc. SICE Annu. Conf.*, 2004, vol. 2, pp. 1696–1701.
- [8] M. Tobias and A. Lanterman, "A probability hypothesis density-based multitarget tracking with multiple bistatic range and Doppler observations," in *Proc. Inst. Electr. Eng. Radar Sonar Navigation*, 2005, vol. 152, pp. 195–205.
- [9] D. Clark and J. Bell, "Bayesian multiple target tracking in forward scan sonar images using the PHD filter," in *Proc. Inst. Electr. Eng. Radar Sonar Navigation*, 2005, vol. 152, pp. 327–334.
- [10] M. Vihola, "Random sets for multitarget tracking and data association," Licentiate, Dept. Inf. Technol. Inst. Math., Tampere Univ. Technol., Finland, 2004.
- [11] O. Erdinc, P. Willett, and Y. Bar-Shalom, "Probability hypothesis density filter for multitarget multisensor tracking," in *Proc. 8th Int. Conf. Inf. Fusion*, 2005, CD-ROM.

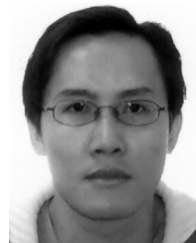
- [12] D. Clark and J. Bell, "Data association for the PHD filter," in *Proc. Int. Conf. Intell. Sens., Sensor Netw. Inf. Process.*, 2005, pp. 217–222.
- [13] K. Panta, B. Vo, and S. Singh, "Improved PHD filter for multitarget tracking," in *Proc. Int. Conf. Intell. Sens. Inf. Process.*, Bangalore, India, 2005, pp. 213–218.
- [14] E. Biglieri and M. Lops, "Multiuser detection in a dynamic environment—Part I: User identification and data detection," *Proc. EUSIPCO*, 2006, CD-ROM.
- [15] D. Clark and J. Bell, "Convergence results for the particle PHD filter," *IEEE Trans. Signal Process.*, vol. 54, no. 7, pp. 2652–2661, Jul. 2006.
- [16] A. Johansen, S. Singh, A. Doucet, and B. Vo, "Convergence of the SMC implementation of the PHD filter," *Methodol. Comput. Appl. Probab.*, vol. 8, no. 2, pp. 265–291, 2006.
- [17] D. Clark and B. Vo, "Convergence analysis of the Gaussian mixture PHD filter," *IEEE Trans. Signal Process.*, vol. 55, no. 4, pp. 1204–1212, Apr. 2006.
- [18] W. K. Ma, B. Vo, S. Singh, and A. Baddeley, "Tracking an unknown and time-varying number of speakers using TDOA measurements: A random finite set approach," *IEEE Trans. Signal Process.*, vol. 54, no. 9, pp. 3291–3304, Sep. 2006.
- [19] A. Pasha, B. Vo, H. Tuan, and W.-K. Ma, "Closed form solution to the PHD recursion for jump Markov linear models," in *Proc. 9th Int. Conf. Inf. Fusion*, 2006, CD-ROM.
- [20] G. Pulford, "Taxonomy of multiple target tracking methods," in *Inst. Electr. Eng. Proc. Radar Sonar Navig.*, 2005, vol. 152, pp. 291–304.
- [21] D. Clark, B. Vo, and J. Bell, "GM-PHD filter multitarget tracking in sonar images," *Proc. SPIE Signal Process., Sensor Fusion, Target Recognit. XV*, vol. 6235, 2006, 62350R.
- [22] K. Panta, B. Vo, S. Singh, and A. Doucet, "Probability hypothesis density filter versus multiple hypothesis tracking," *Proc. SPIE Signal Process., Sensor Fusion, Target Recognit. XIII*, vol. 5429, pp. 284–295, 2004.
- [23] L. Lin, Y. Bar-Shalom, and T. Kirubarajan, "Data association combined with the probability hypothesis density filter for multitarget tracking," *Proc. SPIE Signal Data Process. Small Targets*, vol. 5428, pp. 464–475, 2004.
- [24] R. Mahler, "A theory of PHD filters of higher order in target number," in *Proc. SPIE Defense Security Symp. Signal Process., Sensor Fusion, Target Recognit. XV*, Apr. 2006, vol. 6235, 62350K.
- [25] R. Mahler, "PHD filters of higher order in target number," *IEEE Trans. Aerosp. Electron. Syst.*, vol. 43, no. 3, Jul. 2007, to be published.
- [26] B. Vo, B. Vo, and A. Cantoni, "The cardinalized probability hypothesis density filter for linear Gaussian multitarget models," in *Proc. 40th Conf. Info. Sci. Syst.*, Mar. 2006, pp. 681–686.
- [27] B. Vo, B. Vo, and A. Cantoni, "Performance of PHD based multitarget filters," in *Proc. 9th Int. Conf. Inf. Fusion*, Jul. 2006, CD-ROM.
- [28] D. Stoyan, D. Kendall, and J. Mecke, *Stochastic Geometry and Its Applications*. New York: Wiley, 1995.
- [29] D. Daley and D. Vere-Jones, *An Introduction to the Theory of Point Processes*. New York: Springer-Verlag, 1988.
- [30] O. Erdinc, P. Willett, and Y. Bar-Shalom, "A physical-space approach for the PHD and CPHD filters," in *Proc. SPIE Defense Security Symp. Signal Process., Sensor Fusion, Target Recognit. XV*, Apr. 2006, vol. 6236, 623619.
- [31] P. Borwein and T. Erdélyi, *Newton's Identities Section I.1.E.2 in Polynomials and Polynomial Inequalities*. New York: Springer-Verlag, 1995.
- [32] J. H. A. Aho and J. Ullman, *The Design and Analysis of Computer Algorithms*. Boston, MA: Addison-Wesley, 1975.
- [33] Y. Bar-Shalom and T. E. Fortmann, *Tracking and Data Association*. San Diego, CA: Academic Press, 1988.
- [34] S. Blackman, *Multiple Target Tracking With Radar Applications*. Norwood, MA: Artech House, 1986.
- [35] O. Schrempf, O. Feiermann, and H. Hanebeck, "Optimal mixture approximation of the product of mixtures," in *Proc. 8th Int. Conf. Inf. Fusion*, Jul. 2005, CD-ROM.
- [36] J. Hoffman and R. Mahler, "Multitarget miss distance via optimal assignment," *IEEE Trans. Syst., Man, Cybern. A*, vol. 34, no. 3, pp. 327–336, May 2004.
- [37] Y. Ruan and P. Willett, "The turbo PMHT," *IEEE Trans. Aerosp. Electron. Syst.*, vol. 40, no. 4, pp. 1388–1398, Oct. 2004.
- [38] J. Collins and J. Uhlmann, "Efficient gating in data association with multivariate distributed states," *IEEE Trans. Aerosp. Electron. Syst.*, vol. 28, no. 3, pp. 909–916, Jul. 1992.

- [39] A. H. Jazwinski, *Stochastic Processes and Filtering Theory*. New York: Academic Press, 1970.
- [40] B. D. Anderson and J. B. Moore, *Optimal Filtering*. Englewood Cliffs, NJ: Prentice-Hall, 1979.
- [41] S. J. Julier and J. K. Uhlmann, "Unscented filtering and nonlinear estimation," *Proc. IEEE*, vol. 92, no. 3, pp. 401–422, Mar. 2004.
- [42] Li X.-R and V. Jilkov, "Survey of maneuvering target tracking," *IEEE Trans. Aerosp. Electron. Syst.*, vol. 39, no. 4, pp. 1333–1364, Oct. 2003.



Ba-Tuong Vo was born in Perth, Australia, in 1982. He received the B.Sc. degree in mathematics and the B.E. degree in electrical engineering, with first class honors, from the University of Western Australia, Crawley, WA, Australia, in 2004. He is currently working towards the Ph.D. degree in electrical engineering at the Western Australian Telecommunications Research Institute, the University of Western Australia.

His research interests include point processes, filtering and estimation, and multiobject tracking.



Ba-Ngu Vo was born in Saigon, Vietnam, in 1970. He received the B.S. degrees jointly in science and electrical engineering, with first class honors, from the University of Western Australia, Crawley, WA, Australia, in 1994 and the Ph.D. degree in electrical engineering from the Curtin University of Technology, Perth, WA, Australia, in 1997.

He has held various research positions in Australia and overseas before joining the Department of Electrical and Electronic Engineering, University of Melbourne, Parkville, Vic., Australia, in 2000,

where he is currently an Associate Professor. His research interests include optimization, signal processing, and stochastic geometry.



Antonio Cantoni (M'74–SM'83–F'98) was born in Soliera, Italy, on 30 October, in 1946. He received the B.E. (first class honors) and Ph.D. degrees in electrical engineering from the University of Western Australia, Nedlands, WA, Australia, in 1968 and 1972, respectively.

He was a Lecturer in Computer Science at the Australian National University, Canberra, Australia, in 1972. He joined the Department of Electrical and Electronic Engineering at the University of Newcastle, Shortland, NSW, Australia, in 1973, where he held the Chair of Computer Engineering until 1986. In 1987, he joined QPSX Communications Ltd, Perth, WA, Australia, as Director of the Digital and Computer Systems Design Section for the development of the DQDB Metropolitan Area Network. From 1987 to 1990, he was also a Visiting Professor in the Department of Electrical and Electronic Engineering at the University of Western Australia, Nedlands, WA, Australia. From 1992 to 1997, he was the Director of the Western Australian Telecommunications Research Institute and Professor of Telecommunications at Curtin University of Technology, Perth, WA, Australia. During this period, he was also the Director of the Cooperative Research Centre for Broad-Band Telecommunications and Networking. From 1997 to 2000, he was Chief Technology Officer of Atmosphere Networks an optical networks startup that he cofounded. Since 2000, he has been Research Director of the Western Australian Telecommunications Research Institute and Professor of Telecommunications at the University of Western Australia. He is currently a consultant to Sensear Pty, Ltd., and Inspire Networks Pty, Ltd. startups that he cofounded. His research interests include adaptive signal processing, electronic system design, phase locked loops, and networking.

Dr Cantoni is a Fellow of the Australian Academy of Technological Sciences and Engineering. He has been an Associate Editor of the IEEE TRANSACTIONS ON SIGNAL PROCESSING.